Applied Mechanics and Materials Vols. 29-32 (2010) pp 2435-2442
Online available since 2010/Aug/13 at www.scientific.net

doi:10.4028/www.scientific.net/AMM.29-32.2435

Multi-criteria Optimal Design of Parallel Manipulators Based on Natural Frequency

B.J. LvP[1, aP], S.J. ZhuP[1, b P]and J.F. XingP[1, cP]

[P1P]Department of Mechanical Engineering, Naval University of Engineering, Wuhan, China

[PaP]lvbangjun@sohu.com, P[bP]lvbangjun@yahoo.cn, P[cP]x13871162349@163.com

Keywords: Gough-Stewart manipulator, natural frequency, optimal design, genetic algorithm (GA), Pareto-optimal set

Abstract. The Stewart manipulator has characteristics of low natural frequency, high cost and large size which make it difficult to obtain optimum performance with high dynamic response. The lowest natural frequency in the total workspace and average of six frequencies at home configuration of Stewart manipulator are introduced as indices to evaluate dynamic stability. Multi-criteria optimal design based on genetic algorithm (GA) was presented synthetically considering the workspace requirement, lowest natural frequency, average frequency and global dimensionally homogeneous Jacobian matrix condition number. An optimal result was obtained through standard GA using penalty function and the Pareto-optimal set was also obtained through parallel selection method.

Introduction

Parallel manipulators are widely accepted as ideal candidate in various applications for their inherent superior properties compared with their counterparts, such as higher rigidity, better positioning accuracy, high load capacity and simpler inverse kinematics. However, the relatively small workspace, complex input-output relationship and singularity problems in workspace advise caution in choosing a design [1].

It is well known that performances of parallel manipulators are heavily dependent upon the choice of the mechanical structure and even more from its dimensioning [2]. An appropriate design of geometric parameters in the early stage is of vital significance. Many scholars have paid close attention to the dimensioning optimum design of parallel manipulators [3-7]. Different indices have been adopted for different applications. Liu [3] proposed to design a 3-DoF purely translational parallel mechanism by optimizing good conditioning workspace, global conditioning index and global stiffness index. Nawratil [4] proposed two new performance indices: an end-effector dependent index defined through operation ellipsoid and an end-effector independent index called control number (CTN). Optimal designs of 6-DoF and 3-DoF parallel manipulators are investigated based on the newly defined indices. Wang [5] proposed an optimal method to expand the bandwidth for the control of large hydraulic Stewart platform. And different methods have been applied. Lou [1] et al. investigated the effective regular workspace of parallel manipulators through controlled random search (CRS) technique which was proved efficient and reliable. Hao [6] proposed an interval analysis-based approach to solve optimal design problems and determined a design parameter space that satisfies all design requirements. Optimum is obtained by sampling the parameter space. Recently, Gao [7] et al. optimized the stiffness and dexterity of Stewart manipulator based on artificial intelligence approaches. Overall, it is apparent that many have concentrated on stiffness and few optimization studies take natural frequency into considerations which was proved as dynamic stability index for Stewart platforms [8]. And the method proposed by Wang was chart-based and did not focus on other constraints like workspace, dexterity, etc.

System Description

A parallel manipulator as shown in Figure 1 is regarded as the Gough-Stewart manipulator which consists of a moving platform, a fixed base and six identical extensible links connecting the fixed base to moving platform. The kinematic chains associated with the six legs, from base to platform, consist of a universal joint (2-DOF), a cylinder, an actuated prismatic joint (1-DOF), a piston, and a spherical joint (3-DOF) attached to the moving platform. The platform has six DOF according to Kutzbach-Gruber formula.

The architecture of such a manipulator can then be fully defined by design variables as shown in Figure 1

$$\boldsymbol{\alpha} = \left[R_p, R_B, \lambda_p, \lambda_B, z_0 \right] \tag{1}$$

where R_p , R_B are the radius of the moving platform and the base, respectively, λ_p, λ_B the half angle between two close attachment points on the platform and on the base, z_0 the height of platform at mid-stroke configuration (home configuration). $\boldsymbol{\alpha} \in \left[\boldsymbol{\alpha}_L, \boldsymbol{\alpha}_U \right]$. $\boldsymbol{\alpha}_L, \boldsymbol{\alpha}_U$ are the lower and upper boundaries of these design variables considering the manufacture and machining factors.

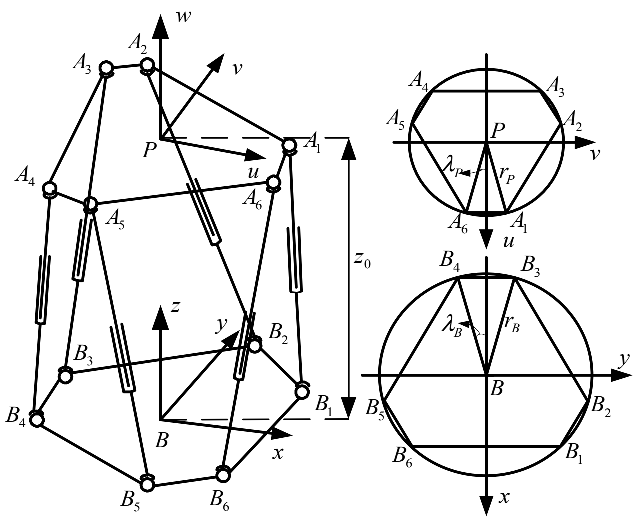

Fig. 1: Schematic and design variables for Gough-Stewart manipulator

Workspace Constraints

When design for parallel manipulators, we are aiming at a desired workspace $\boldsymbol{W}$ where the manipulator can work with no restriction. However, because of mechanical limits on passive joints, interference between links and limitations due to the actuators, not all configurations can be achieved. For Stewart manipulator, $\forall \boldsymbol{X} \in W$, $\boldsymbol{X}$ is an 6 dimensional vector denoted by $\boldsymbol{X} = [x, y, z, \boldsymbol{\varphi}, \boldsymbol{\theta}, \boldsymbol{\psi}]$, where x, y, z represent displacements of the moving reference frame centre P and $\boldsymbol{\varphi}, \boldsymbol{\theta}, \boldsymbol{\psi}$ represent Euler angles of the moving platform. The actuator lengths can be calculated through inverse kinematics and should satisfy

$$L_i^{\min} \le L_i \left(\boldsymbol{X}, \boldsymbol{\alpha} \right) \le L_i^{\max} \quad i = 1, 2, \cdots 6 \tag{2}$$

where $L_i^{\min}$ and $L_i^{\max}$ are the minimum and maximum lengths that can be reached by actuators respectively.

Considering the working boundary of passive joints as shown in Figure 2, the deviation angle of universal joints and spherical joints connecting the upper and lower platform should satisfy

$$\begin{aligned} \varphi_A^{\min} \le \varphi_{Ai}\left(\boldsymbol{X},\alpha\right) \le \varphi_A^{\max} \\ \varphi_B^{\min} \le \varphi_{Bj}\left(\boldsymbol{X},\alpha\right) \le \varphi_B^{\max} \end{aligned} \tag{3}$$

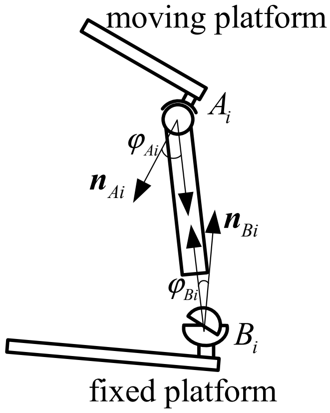

Fig. 2: Deviation angle of passive joints

In addition, because of the complex structure of parallel manipulators, the volume of workspace will be affected by link interference. Assume that the manipulator has t links represented by cylinders with radius of R_i denoted by line segments $\boldsymbol{L}_i$ and notice that $\boldsymbol{L}_i = \boldsymbol{L}_i\left(\boldsymbol{x},\boldsymbol{\alpha}\right)$. There is no link interference if the distance between any pair of line segments is larger than the sum of corresponding radii

$$\text{distance}\left(\boldsymbol{L}_i,\boldsymbol{L}_j\right) \ge R_i + R_j \tag{4}$$

Dimensionally Homogeneous Jacobian Matrix Condition Number

Salisbury and Craig introduced condition number (CDN) of Jacobian matrix to evaluate the dexterity of Stanford/JPL robot hand [9]

$$CDN = \left\|\boldsymbol{J}\right\|_2 \cdot \left\|\boldsymbol{J}^{-1}\right\|_2 \tag{5}$$

However, when manipulators have both translational and rotational dofs, the condition number will not be invariant under scaling of dimensions. Use of the condition number of the Jacobian matrix with nonhomogeneous physic units in the optimal design or control may cause significant problems [11]. Kim and Ryu presented a new formulation of a dimensionally homogenous Jacbobian matrix for parallel manipulators with a planar mobile platform by using three end-effector points that are coplanar with the mobile platform joint. The dimensionally homogeneous Jacobian matrix has the form [10] [11]

$$\tilde{\boldsymbol{J}} = \begin{bmatrix} \dfrac{\partial l_1}{\partial A_{1x}} & \dfrac{\partial l_1}{\partial A_{1y}} & \dfrac{\partial l_1}{\partial A_{2x}} & \dfrac{\partial l_1}{\partial A_{2y}} & \dfrac{\partial l_1}{\partial A_{3x}} & \dfrac{\partial l_1}{\partial A_{3y}} \\ \dfrac{\partial l_2}{\partial A_{1x}} & \dfrac{\partial l_2}{\partial A_{1y}} & \dfrac{\partial l_2}{\partial A_{2x}} & \dfrac{\partial l_2}{\partial A_{2y}} & \dfrac{\partial l_2}{\partial A_{3x}} & \dfrac{\partial l_2}{\partial A_{3y}} \\ & & \vdots & \vdots & & \\ \dfrac{\partial l_6}{\partial A_{1x}} & \dfrac{\partial l_6}{\partial A_{1y}} & \dfrac{\partial l_6}{\partial A_{2x}} & \dfrac{\partial l_6}{\partial A_{2y}} & \dfrac{\partial l_6}{\partial A_{3x}} & \dfrac{\partial l_6}{\partial A_{3y}} \end{bmatrix}_{6\times 6} \tag{6}$$

where A_{ix}, A_{iy} $(i=1,2,3)$ are the x and y coordinates of three end-effector points in fixed reference frame.

And the dexterity index as

$$\eta_1 = \kappa(\tilde{\boldsymbol{J}}) = \left\|\tilde{\boldsymbol{J}}\right\|_2 \cdot \left\|\tilde{\boldsymbol{J}}^{-1}\right\|_2 = \sqrt{\lambda_{\max}\left(\tilde{\boldsymbol{J}}^T\tilde{\boldsymbol{J}}\right) \big/ \lambda_{\min}\left(\tilde{\boldsymbol{J}}^T\tilde{\boldsymbol{J}}\right)} \tag{7}$$

where $\lambda_{\max}(\cdot)$ and $\lambda_{\min}(\cdot)$ represent the maximum and minimum eigenvalue of matrix. It's obviously that $1 \le \kappa(\tilde{\boldsymbol{J}}) < \infty$. When $\kappa(\tilde{\boldsymbol{J}})$ equals 1, the manipulator is of optimal motion transfer capability and called an isotropy manipulator in this configuration. $\kappa(\tilde{\boldsymbol{J}})$ is configuration dependent and when $\kappa(\tilde{\boldsymbol{J}})$ becomes huge, the manipulator may approach a singularity configuration.

Natural Frequency Index

The complete dynamic equations of 6-UPS Stewart platform in general form in Cartesian space

$$\boldsymbol{M}(\boldsymbol{q})\ddot{\boldsymbol{q}} + \boldsymbol{C}(\boldsymbol{q},\dot{\boldsymbol{q}})\dot{\boldsymbol{q}} + \boldsymbol{G}(\boldsymbol{q}) = \boldsymbol{J}_p^T\boldsymbol{F} \tag{8}$$

From the principle of virtual work and the definition of the Jacobian matrix, we obtained the following relationship between the joint torques and the force applied to the end-effector

$$\boldsymbol{\tau} = \boldsymbol{J}_P^T\boldsymbol{F} \tag{9}$$

When manipulator is under free vibration

$$\boldsymbol{\tau} = -\boldsymbol{K}_c\delta\boldsymbol{x} \tag{10}$$

where $\delta\boldsymbol{x}$ represents the configuration vector of the moving platform.

The Cartesian stiffness matrix of Stewart mechanism

$$\boldsymbol{K}_C = \boldsymbol{J}_p^T\boldsymbol{K}\boldsymbol{J}_p \tag{11}$$

where $\boldsymbol{K} = diag([k_1, k_2, \cdots k_6])$, k_i is the equivalent axial linear stiffness of each branch.

Free vibration of the platform around any equilibrium configuration is governed by the following linear perturbation equation

$$\boldsymbol{M}_1\delta\ddot{\boldsymbol{x}} + \boldsymbol{K}_c\delta\boldsymbol{x} = 0 \tag{12}$$

where $\boldsymbol{M}_1 = \boldsymbol{M}(\boldsymbol{q}) \cdot \begin{bmatrix} \boldsymbol{E} & 0_{3\times3} \\ 0_{3\times3} & \boldsymbol{H} \end{bmatrix}$, $\boldsymbol{H} = \begin{bmatrix} \cos(\psi)\cos(\theta) & -\sin(\psi) & 0 \\ \sin(\psi)\cos(\theta) & \cos(\psi) & 0 \\ -\sin(\theta) & 0 & 1 \end{bmatrix}$ considering the relationship between the platform angular acceleration and the first and second derivatives of Euler angles.

Assume $\delta\boldsymbol{x} = \boldsymbol{X}e^{i\omega t}$ to be a solution of Eqution 12, we get the generalized eigenvalue problem as

$$\left(\boldsymbol{K}_C - \omega^2\boldsymbol{M}_1\right)\boldsymbol{X} = 0 \tag{13}$$

The system has non-trivial solution if coefficient matrix vanishes and the eigenvalue equation is obtained

$$\det\left(\boldsymbol{K}_C - \omega^2 \boldsymbol{M}_1\right) = 0 \tag{14}$$

Solving Eqution 13and 14, we get six natural frequencies and corresponding modal vectors for the Stewart platform in a particular configuration. Both kinematic and dynamic effects are included in natural frequencies. The manipulator dynamic stability will gradually decrease if the lowest natural frequency falls, and finally become highly unstable when the lowest natural frequency get close to zero and, therefore, can not restore the configuration if it is perturbed by any amount. Thus, the lowest natural frequency, calculated from Eqution 14 can be taken as index for dynamic stability.

For Stewart platforms, the key frequencies are the lowest natural frequency in the total workspace and the generalized natural frequency at the mid-stoke configuration (home configuration) [5] considering that the platform is mostly working around its home configuration.

$$\eta_2 = \min_W \omega(\boldsymbol{X}, \boldsymbol{\alpha}) \tag{15}$$

$$\eta_3 = \frac{1}{6}\sum_{i=1}^{6} \omega_{ic} \tag{16}$$

where $\omega_{ic}\ (i = 1, 2\cdots 6)$ are six natural frequencies at the home configuration of Stewart platform.

Optimizing Model

The optimizing model base on natural frequencies and dexterity can be obtained

$$\begin{cases} \min A(\boldsymbol{\alpha}) = w_1\eta_1(\boldsymbol{X},\boldsymbol{\alpha}) + w_2\eta_2(\boldsymbol{X},\boldsymbol{\alpha}) + w_3\eta_3(\boldsymbol{X},\boldsymbol{\alpha}) \\ s.t.\ \boldsymbol{\alpha}_{\mathrm{L}} \le \boldsymbol{\alpha} \le \boldsymbol{\alpha}_U \\ L_i^{\min} \le L_i(\boldsymbol{X},\boldsymbol{\alpha}) \le L_i^{\max} \\ \varphi_k^{\min} \le \varphi_k(\boldsymbol{X},\alpha) \le \varphi_k^{\max} \\ \mathrm{distance}\left(\boldsymbol{L}_i, \boldsymbol{L}_j\right) \ge R_i + R_j \end{cases} \tag{17}$$

where $w_{1,2,3}$ are weighting factors of different objective function values and $\sum_{i=1}^{3} w_i = 1$. Then the multi-objective optimization problem transformed into single-objective optimization.

Simulation Results

Eqution 17 is clearly a constrained, nonlinear, multi-objective optimization problem. Three indices in Eqution 7, 15 and 16 as well as the constraints have no explicitly analytical expressions with respect to the set of design variables. Traditional gradient-based methods may not be appropriate in this problem. Fortunately, Genetic algorithm (GA) can be applied to solve a variety of optimization problems that are not well suited for standard optimization algorithm, including problems in which the objective function is discontinuous, non-differentiable, stochastic, or highly nonlinear, since GA is a global method for solving both constrained and unconstrained optimization problems based on natural evolution. In this section, two optimization examples are investigated here to demonstrate the design procedure.

First, a weighting factor based typical genetic algorithm is introduced in simulation. The lower and upper boundaries of these design variables are restricted as: $\boldsymbol{\alpha}_L = \left[0.05\mathrm{m}, 0.12\mathrm{m}, 18^\circ, 12^\circ, 0.16\mathrm{m}\right]$, $\boldsymbol{\alpha}_U = \left[0.1\mathrm{m}, 0.22\mathrm{m}, 28^\circ, 22^\circ, 0.26\mathrm{m}\right]$. The workspace are prescribed as: moving workspace

$-0.05 \le x \le 0.05$, $-0.05 \le y \le 0.05$, $-0.05 \le z \le 0.05$ when $\varphi = 0, \theta = 0, \psi = 0$, rotating workspace $-15^\circ \le \varphi \le 15^\circ$, $-15^\circ \le \theta \le 15^\circ$, $-20^\circ \le \psi \le 20^\circ$ when $x = 0, y = 0, z = 0$.

For GA application, the fitness function should be monotone, non-negative and continuous which can be transformed from object function Eqution 17 as

$$F(\boldsymbol{\alpha}) = C_{\max} - A(\boldsymbol{\alpha}) - g\sum_{i=1}^{m}\left(\left|h_i(\boldsymbol{X},\boldsymbol{\alpha})\right| + h_i(\boldsymbol{X},\boldsymbol{\alpha})\right) \tag{18}$$

where $C_{\max}$ is an estimated maximum value to ensure the positive of $F(\boldsymbol{\alpha})$, $h_i(\boldsymbol{X},\boldsymbol{\alpha}) \le 0$ are transformed from constraints in Eqution 17, for example $L_i^{\min} \le L_i(\boldsymbol{X},\boldsymbol{\alpha}) \le L_i^{\max}$ can be transformed as $L_i^{\min} - L_i(\boldsymbol{X},\boldsymbol{\alpha}) \le 0$ and $L_i(\boldsymbol{X},\boldsymbol{\alpha}) - L_i^{\max} \le 0$. g is a positive penalty factor to sharply decrease fitness value when constraints are not satisfied i.e. $h_i(\boldsymbol{X},\boldsymbol{\alpha}) > 0$. Weighting factors in Eqution 17 are choosing as: $w_1 = 0.2, w_2 = 0.5, w_3 = 0.3$.

Best solution maintaining principle was adopted during the searching procedure to get a fast convergent speed. Figure 3 and 4 show that after 20 generations, the design parameters are convergent at

$$\boldsymbol{\alpha} = \left[R_p, R_B, \lambda_p, \lambda_B, z_0\right] = [0.1, 0.22, 0.48869, 0.38397, 0.16]$$

and the objective function $A(\boldsymbol{\alpha}) = 4.7254$

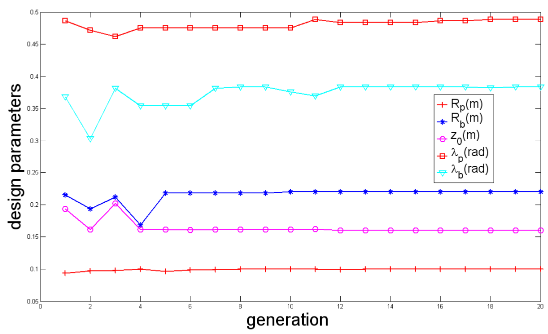

Fig. 3: The evolution of architecture parameters in standard GA

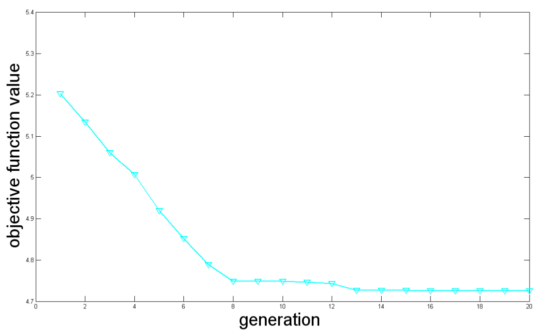

Fig. 4: The evolution of fitness function in standard GA

However, in practice the objective functions usually conflict with each other [7] and the optimal result is sensitive to weighting factors which makes it difficult to make compromise between different requirements. In the following section, a Pareto-set based optimization without factor choosing is investigated and the Pareto-optimal set can be obtained through parallel selection GA. On the contrary to standard GA, each sub-population corresponds to a fitness function in selection step and all sub-populations are recombined after selection.

The following initial parameters of the Pareto-based genetic algorithms are created:

Numbers of sub-populations: 5

Numbers of chromosome in each sub- population: 50

Mutation rate: 0.1

Crossover rate: 0.7

Maximum generations for GA: 200

Figure 5 shows the Pareto-optimal frontier in spatial space after 200 generations, where designers can make decisions by sampling the corresponding Pareto-optimal set according to their experiences or preferences. Figure 6 shows the vertical view of the Pareto-frontier where the lower-left area is beyond the frontier and inaccessible in the solution space, while sampling in the upper-right area of the frontier can only obtain an inferior solution where either minimum frequency or condition number is larger than the Pareto-optimal points.

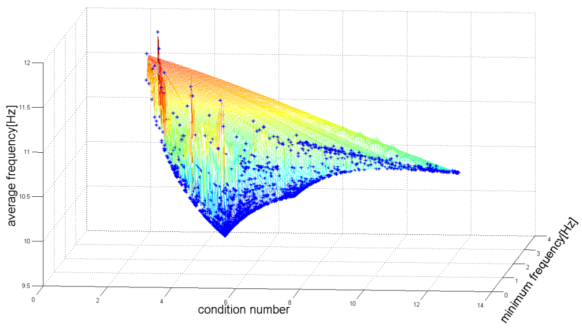

Fig. 5: Pareto-frontier in the solution space

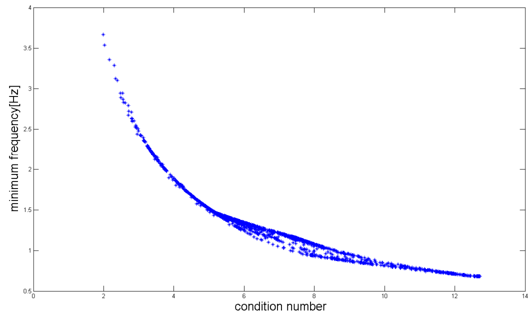

Fig. 6: Pareto-frontier in the solution space (vertical view)

Conclusion

In this paper, GA based optimizations have been investigated in order to increase the dynamic stability of Gough-Stewart parallel manipulator. Three indices, including the minimum natural frequency in the workspace, average natural frequency at home configuration and dimensionally homogeneous Jacobian matrix condition number, are introduced as objective functions in multi-objective design.

The weighting factor method is adopted to transfer the multi-objective optimization to single-objective by setting a set of factors to make compromise between conflicting demands. An optimal design can be obtained quickly through standard GA. The Pareto-set based optimization is also investigated through parallel selection GA, and a Pareto-optimal frontier is gained in spatial space. And the design procedure becomes sampling the corresponding Pareto-optimal set which may be more practical available for designers.

References

[1] Y.J. Lou, G.F. Liu, Z.X. Li, "Optimal Design of Parallel Manipulators via LMI Approach", *Proceedings of IEEE International Conference on Robotics and Automation*, Vol. 2, pp. 1869-1874, 2003.

[2] J.P. Merlet, D. Daney, "Appropriate Design of Parallel Manipulators", *Smart Devices and Machines for Advanced Manufacturing*, Springer, London, 2008.

[3] X.J. Liu, "Optimal kinematic design of a three translational DoFs parallel manipulator", *Robotica*, Vol.24, No.2, pp. 239-250, 2006.

[4] G. Nawratil, "New performance indices for 6-dof UPS and 3-dof RPR parallel manipulators", *Mechanism and Machine Theory*, Vol.44, No.1, pp. 208-221, 2009.

[5] W. Wang, H.Y. Yang, J. Zou, et al, "Optimal design of Stewart platforms based on expanding the control bandwidth while considering the hydraulic system design", *Journal of Zhejiang University Science A*, Vol.10, No.1, pp. 1862-1775, 2009.

[6] F. Hao, J.P. Merlet, "Multi-criteria optimal design of parallel manipulators based on interval analysis", *Mechanism and Machine Theory*, Vol.40, No.2, pp. 157-171, 2005.

[7] Z. Gao, D. Zhang, Y.J. Ge, "Design optimization of a spatial six degree-of-freedom parallel manipulator based on artificial intelligence approaches", *Robotics and Computer-Integrated Manufacturing*, Vol.26, No.2, pp. 180-189, 2010.

[8] P. Mukherjee, B. Dasgupta, A.K. Mallik, "Dynamic stability index and vibration analysis of a flexible Stewart platform", *Journal of sound and vibration*, Vol.307, No.3-5, 495-512, 2007.

[9] J.K. Slisbury, J.J. Craig, "Articulated hands: force control and kinematic issues", *International Journal of Robotics Research*, Vol.1, No.1, pp. 4-17, 1982.
[10] G. Pond, J.A. Carretero, "Formulating Jacobian matrices for the dexterity analysis of parallel manipulators", *Mechanism and Machine Theory*, Vol.41, No.12, pp. 1505-1519, 2006.
[11] S.G. Kim, J. Ryu, "New dimensionally homogeneous jacobian matrix formulation by three end-effector points for optimal design of parallel manipulators", *IEEE Transactions on Robotics and Automation*, Vol.19, No.4, pp. 731-736, 2003.

Applied Mechanics And Mechanical Engineering
10.4028/www.scientific.net/AMM.29-32

Multi-Criteria Optimal Design of Parallel Manipulators Based on Natural Frequency
10.4028/www.scientific.net/AMM.29-32.2435

DOI References

[3] X.J. Liu, “Optimal kinematic design of a three translational DoFs parallel manipulator”, obotica, Vol.24, No.2, pp. 239-250, 2006.
doi:10.1017/S0263574705002079
[5] W. Wang, H.Y. Yang, J. Zou, et al, “Optimal design of Stewart platforms based on expanding the ontrol bandwidth while considering the hydraulic system design”, Journal of Zhejiang niversity Science A, Vol.10, No.1, pp. 1862-1775, 2009.
doi:10.1631/jzus.A0820329
[6] F. Hao, J.P. Merlet, “Multi-criteria optimal design of parallel manipulators based on interval nalysis”, Mechanism and Machine Theory, Vol.40, No.2, pp. 157-171, 2005.
doi:10.1016/j.mechmachtheory.2004.07.002
[8] P. Mukherjee, B. Dasgupta, A.K. Mallik, “Dynamic stability index and vibration analysis of a lexible Stewart platform”, Journal of sound and vibration, Vol.307, No.3-5, 495-512, 2007.
doi:10.1016/j.jsv.2007.05.036
[10] G. Pond, J.A. Carretero, “Formulating Jacobian matrices for the dexterity analysis of parallel anipulators”, Mechanism and Machine Theory, Vol.41, No.12, pp. 1505-1519, 2006.
doi:10.1016/j.mechmachtheory.2006.01.003
[3] X.J. Liu, “Optimal kinematic design of a three translational DoFs parallel manipulator”, Robotica, Vol.24, No.2, pp. 239-250, 2006.
doi:10.1017/S0263574705002079
[4] G. Nawratil, “New performance indices for 6-dof UPS and 3-dof RPR parallel manipulators”, Mechanism and Machine Theory, Vol.44, No.1, pp. 208-221, 2009.
doi:10.1016/j.mechmachtheory.2008.02.004
[5] W. Wang, H.Y. Yang, J. Zou, et al, “Optimal design of Stewart platforms based on expanding the control bandwidth while considering the hydraulic system design”, Journal of Zhejiang University Science A, Vol.10, No.1, pp. 1862-1775, 2009.
doi:10.1631/jzus.A0820329
[6] F. Hao, J.P. Merlet, “Multi-criteria optimal design of parallel manipulators based on interval analysis”, Mechanism and Machine Theory, Vol.40, No.2, pp. 157-171, 2005.
doi:10.1016/j.mechmachtheory.2004.07.002
[7] Z. Gao, D. Zhang, Y.J. Ge, “Design optimization of a spatial six degree-of-freedom parallel manipulator based on artificial intelligence approaches”, Robotics and Computer-Integrated Manufacturing, Vol.26, No.2, pp. 180-189, 2010.
doi:10.1016/j.rcim.2009.07.002
[8] P. Mukherjee, B. Dasgupta, A.K. Mallik, “Dynamic stability index and vibration analysis of a flexible Stewart platform”, Journal of sound and vibration, Vol.307, No.3-5, 495-512, 2007.
doi:10.1016/j.jsv.2007.05.036

[10] G. Pond, J.A. Carretero, “Formulating Jacobian matrices for the dexterity analysis of parallel manipulators”, Mechanism and Machine Theory, Vol.41, No.12, pp. 1505-1519, 2006. doi:10.1016/j.mechmachtheory.2006.01.003